PHOTONIC SENSORS / Vol. 7, No. 2, 2017: 163–170

Effect of Radio Frequency Magnetron Sputtering Power on Structural and Optical Properties of Ti6Al4V Thin Films

Mohammed K. KHALAF[1*], H. F. Al-TAAY[2], and Dawood S. ALI[3]

[1] *Ministry of Science and Technology, Center of Applied Physics, Baghdad, Iraq*

[2]*Department of Physics, College of Science for Women, University of Baghdad, Baghdad, Iraq*

[3]*Department of Physics, College of Education for Pure Sciences, University of Anbar, Anbar, Iraq*

[*]Corresponding author: Mohammed K. KHALAF E-mail: mohammedkhkh@yahoo.com

Abstract: In this research, the effects of target sputtering power on the structure and optical properties of radio frequency (RF) sputtered Ti6Al4V films were investigated. Different sputtering RF powers were used to produce different thicknesses of Ti6Al4V thin films. From the X-ray diffraction, it was found that the Ti6A14V films had polycrystalline cubic and hexagonal structures and increased films crystallinity and crystalline size with increasing the sputtering power. Atomic forces microscopy (AFM) gave us a nanometric film character, films homogeneity, and surfaces roughness. A higher degree of roughness and average grain size with increasing RF power was exhibited. Band gap and refractive index of Ti6Al4V thin films varied with sputtering RF powers.

Keywords: RF magnetron sputtering; Ti6Al4V; structural properties; optical properties.

Citation: Mohammed K. KHALAF, H. F. Al-TAAY, and Dawood S. ALI, "Effect of Radio Frequency Magnetron Sputtering Power on Structural and Optical Properties of Ti6Al4V Thin Films," *Photonic Sensors*, 2017, 7(2): 163–170.

1. Introduction

Due to the interesting chemical and mechanical properties, the titanium alloy is far used in many applications [1, 2]. One particular alloy, the Ti6Al4V, has the most performance among the different grades of titanium. The Ti6Al4V thin films have attracted large scientific and practical interest since their specific properties enable various applications as microstructure materials in surgical appliances [3, 4]. The pure titanium is a monophasic, physiologically inert, and non-toxic metal. Ternary titanium alloys containing Al and V exhibit α and β phases structure that has attractive mechanical properties, high wear resistance, hardness, tenacity, resistance to fatigue, and high corrosion resistance [5]. Besides having a low density, it has an excellent biocompatibility of permitting its use in the fabrication of medical implants [6]. There are many deposition methods used to prepare Ti6Al4V, by means of chemical vapor deposition (CVD) [7], electrochemical method [8], selective laser melting [9], and physical vapor deposition (PVD) such as RF-DC sputtering [10]. In this work, Ti6Al4V thin films have been deposited on glass substrates by the radio frequency (RF) magnetron sputtering method with five different deposition power conditions. The crystallographic properties and surface morphology of the films were studied by the X-ray diffraction (XRD) and atomic forces microscopy (AFM)

Received: 2 November 2016 / Revised: 7 January 2017

DOI: 10.1007/s13320-017-0390-8
Article type: Regular

techniques. The optical property measurements for Ti6Al4V thin films are obtained by using the UV (ultraviolet) -visible recording spectrometer.

2. Experiment

In our study, Ti6Al4V thin films were prepared by using the RF magnetron sputtering technique (CRC600 CO.USA-made). The thin films were deposited on the glass substrate with different powers. The glass slides were sequentially cleaned in an ultrasonic bath with acetone and ethanol. Finally, they were rinsed with distilled water and dried. The sputtering chamber was evacuated to 5×10^{-5} mbar base pressure using diffusion and mechanical booster pump combination prior to the deposition. Before the deposition of Ti6Al4V films, a Ti6Al4V target (99.99% pure and 5 cm diameter) was pre-sputtered in pure argon atmosphere for 10 min in order to remove oxide on the surface of the target. Ti6Al4V films were deposited by the RF sputtering system in pure argon gas (99.9%) with pressure of 5×10^{-2} mbar. The X-ray diffraction measurements of thin films were performed by using the diffract meter type (SHIMADZU-6000). The AFM was a contact mode used to analyze the morphological feature on Angstrom Inc. (AA3000). The optical properties measurements for Ti6Al4V thin films were obtained by using the UV-Visible recording spectrometer (UV-2601 PC Shimadzu software 1700 1650). The thickness of the films has been calculated by using the Device FT-650 Film Thickness (FT) Probe System.

3. Results and discussion

3.1 X-ray diffraction (XRD)

It can be expected that low sputtering power exhibits a low deposition rate which is due to less energetic argon over the target species and less ejected atoms from the target material. However, when the sputtering power was increased, the sputtering yield of the Ti6Al4V films markedly was increased. Figure 1 shows the XRD analysis for Ti6A14V thin films deposited on glass substrates with different powers (50 W, 75 W, 100 W, 125 W, and 150 W, respectively). The XRD pattern illustrates that the Ti6A14V films had a polycrystalline structure with peaks attributed to (110) diffractions for cubic structure or (002) diffractions for hexagonal structure and (102) diffractions for cubic structure, identified with standard peaks (card No. 96-900-8555 and 96-900-8518). Also, note that an increase in the RF power led to an increase in the peak intensity (i.e. an increase in films crystallinity). The mobility improvement of adatoms sputtered on the surface, which was required to form highly crystalline films. Because it is believed that high DC sputtering power in the magnetron sputtering system energizes inert argon gas to provide sufficient kinetic energy to adatoms, the surface diffusion of these adatoms was then expected to enhance with the momentum transfer to the nucleation and growth of the Ti6Al4V films. Increasing the RF power will make an increase in the grain size, as shown in Table 1. This may be due to the enhancement of crystallinity in the films. The films of crystalline was improved which led to a decrease in the number of grain boundaries. A significant line was broadened which is a characteristic of nanoparticles [1, 11].

Table 1 Comparison between the Exp. and Std. the values of d_{hkl} for the (Ti6Al4V) peaks shown in XRD for different RF powers on a glass substrate.

Power (W)	2θ(deg.)	β (FWHM) (deg.)	d_{hkl} Exp.(Å)	G.S (nm)	d_{hkl} Std.(Å)	Phase	hkl
50	38.4010	1.7020	2.3422	4.9	2.3380	Cubic	(110)
					2.3430	Hex.	(002)
	53.8120	1.6503	1.7022	5.4	1.7268	Hex.	(102)
75	38.5902	0.9230	2.3312	9.1	2.3380	Cubic	(110)
					2.3430	Hex.	(002)
	53.7980	1.4120	1.7026	6.3	1.7268	Hex.	(102)
100	38.4320	0.6013	2.3404	14.0	2.3380	Cubic	(110)
					2.3430	Hex.	(002)
	53.8210	0.9340	1.7020	9.5	1.7268	Hex.	(102)
125	38.4610	0.5780	2.3387	14.6	2.3380	Cubic	(110)
					2.3430	Hex.	(002)
	53.7650	1.1043	1.7036	8.1	1.7268	Hex.	(102)
150	38.4426	0.5431	2.3398	15.5	2.3380	Cubic	(110)
					2.3430	Hex.	(002)
	53.7630	0.5312	1.7037	16.8	1.7268	Hex.	(102)

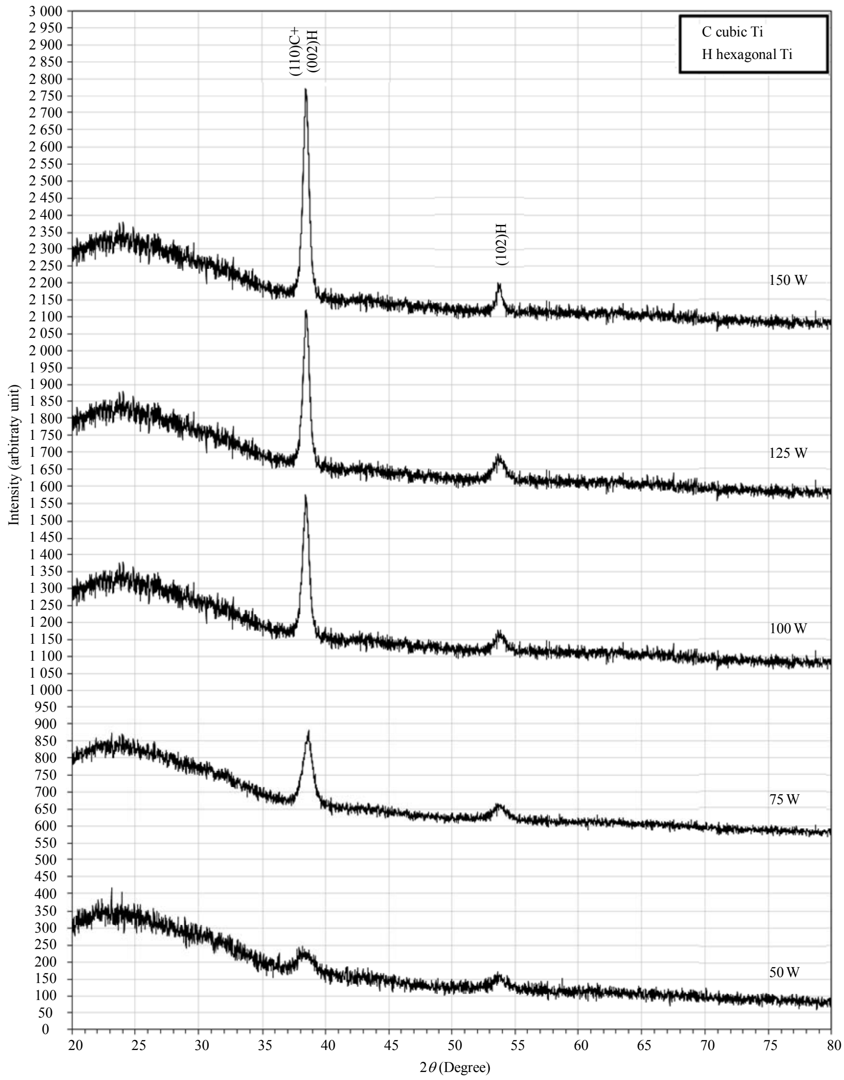

Fig. 1 X-ray diffraction patterns of the (Ti6A14V) films deposited on the glass substrate at different sputtering powers.

3.2 Atomic force microscope

The surface morphology of Ti6Al4V films deposited on the glass substrate was studied by AFM to monitor the growth of nanostructure under the influence of different deposition powers. Figure 2 shows 2D and 3D AFM images of Ti6Al4V thin film deposited at different working sputtering powers. The images have light and dark regions. From the colors, brightness is used to specify the vertical profile of the thin film surface, where light regions represent the highest points and the dark points are the depressions. This figure confirms that the films are uniform, and the substrate surface is well covered with grains that are nearly uniformly distributed. From these images, it is observed that the surfaces of the films exhibit more degree of roughness with increasing the RF power. In addition, an increase in the average grain size leads to an increase in the root mean square roughness (RMS), as shown in Table 2. The Ti6Al4V film deposited at higher sputtering power exhibits profound large grains with orientations. These morphologies are due to the fact that sputtering power helps increase the surface mobility of adatoms, which is required to form continuous films. The surface diffusion of these adatoms is then enhanced by the higher sputtering power, which results in a provision of the momentum transfer to the growing surface.

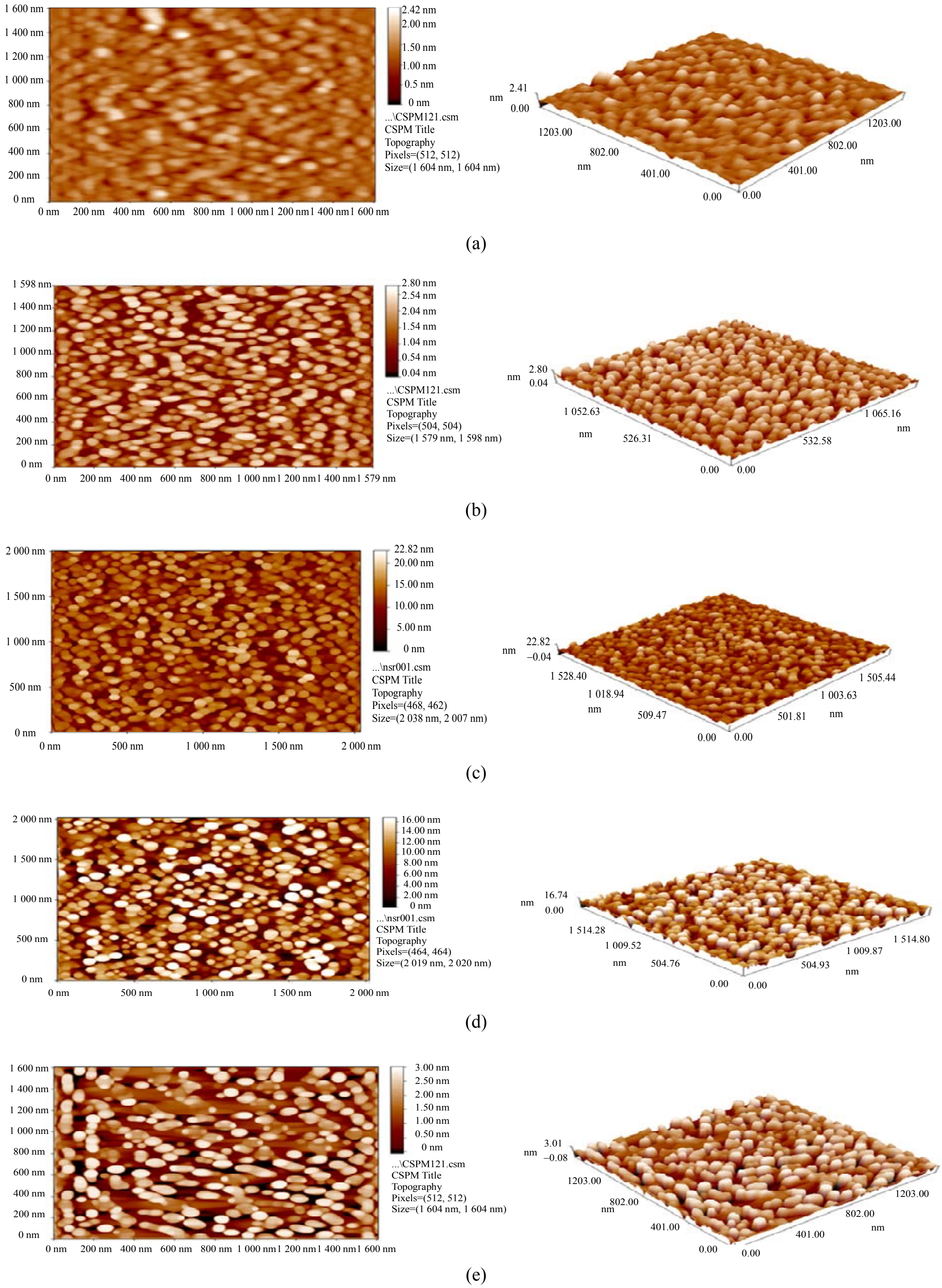

Fig. 2 Two-dimensional (2D) and three-dimensional (3D) AFM images of (Ti6Al4V) thin films deposited on glass substrate at different RF powers: (a) 50 W, (b) 75 W, (c) 100 W, (d) 125 W, and (e) 150 W.

Table 2 AFM data of (Ti6Al4V) thin films deposited on the glass substrate at different RF powers.

Power (W)	Average diameter of granularity (nm)	Root mean square roughness (nm)	Average roughness (nm)
50	50.21	0.255	0.190
75	57.38	0.569	0.487
100	75.38	0.848	0.730
125	81.70	3.320	2.710
150	92.85	4.000	3.340

3.3 Optical measurements

The optical properties of the Ti6Al4V thin films deposited by RF magnetron sputtering were analyzed by UV-visible spectroscopy in the wavelength range of 400 nm–1100 nm as shown in Fig. 3. The transmission spectra of Ti6Al4V thin film at different RF powers (50 W, 75 W, 100 W, 125 W, and 150 W) decrease with an increase in RF power when films thicknesses increase (244.89 nm, 435.26 nm, 598.98 nm, 866.23 nm, and 910.46 nm, respectively). The transmittance patterns of all deposited thin films on glass increase with an increase in wavelength (λ). A decrease in the transmittance spectra is caused by an increase in the loss of light scattering as the grain size increases [12].

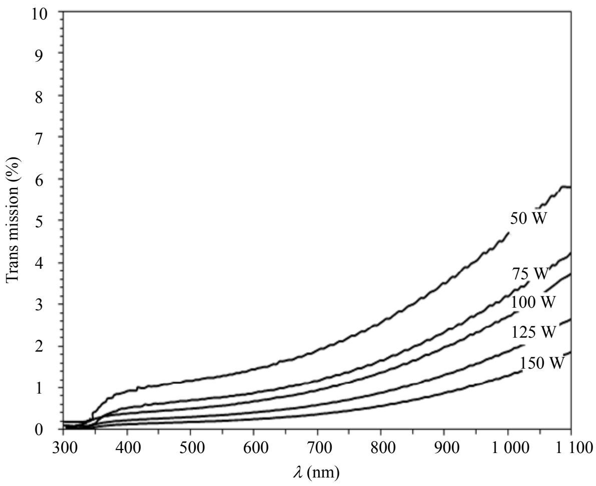

Fig. 3 Transmittance as a function of wavelength for (Ti6Al4V) thin film at different working RF powers.

Absorbance spectra of Ti6Al4V thin films at different RF powers are shown in Fig. 4. An increase in absorbance due to a decrease in transmission associates with a change in the thickness. The figure shows that the optical absorption in the UV region is high. The absorption patterns of all deposited thin films on glass decrease with an increase in the wavelength.

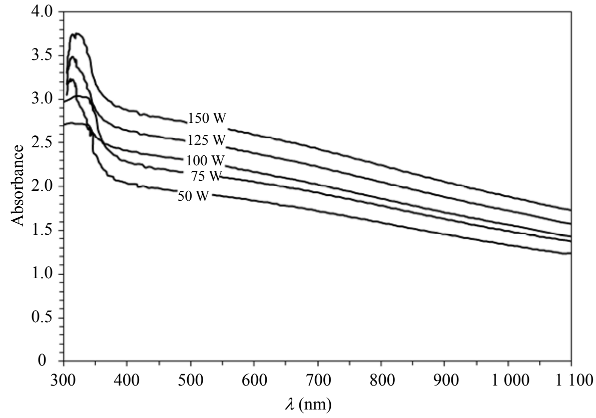

Fig. 4 Absorbance as a function of wavelength for (Ti6Al4V) thin film at different working RF powers.

Figure 5 displays the absorption coefficient as a function of wavelength for Ti6Al4V thin films deposited at different RF powers. The absorption coefficient increases with an increase in the film thickness which is proportional to RF power. Also, the absorption coefficient of deposited thin films on glass decreases with an increase in the wavelength.

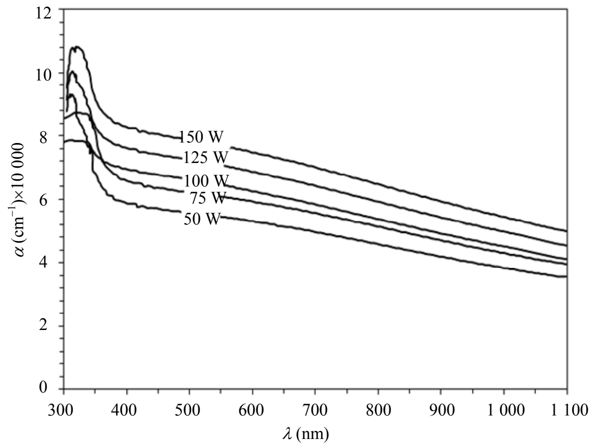

Fig. 5 Absorption coefficient as a function of wavelength for (Ti6Al4V) thin film at different working RF powers.

Figure 6 illustrates the variation of extinction coefficient with wavelength in the range of 400 nm–1100 nm for Ti6Al4V films deposited on the glass substrate at different RF powers. The extinction coefficient depends mainly on the absorption coefficient, and we notice that the extinction coefficient decreases with an increase in the wavelength because of the increment in the absorption coefficient [13].

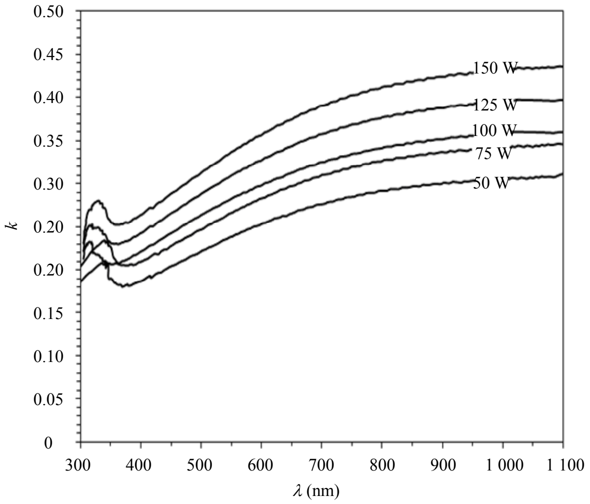

Fig. 6 Extinction coefficient as a function of wavelength for (Ti6Al4V) thin film at different working RF powers.

Figures 7 and 8 show the dielectric constant and dielectric loss as a function of wavelength for Ti6Al4V thin films deposited at different RF powers. The dielectric constants decrease with an increase in RF power and increase with an increase in the wavelength (λ). The variation of the dielectric constant depends on the value of the refractive index. By contrast, the dielectric loss depends mainly on the extinction coefficient values which are related to the variations of absorption [13].

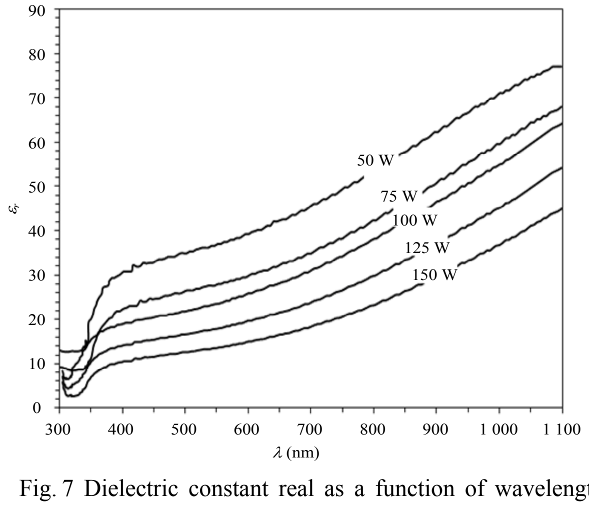

Fig. 7 Dielectric constant real as a function of wavelength for (Ti6Al4V) thin film at different working RF powers.

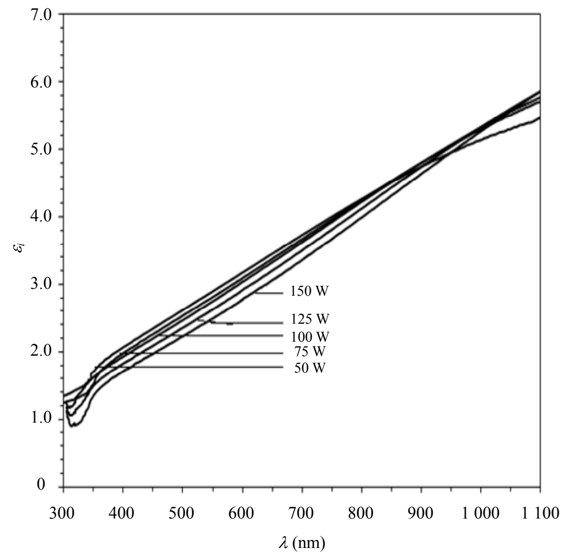

Fig. 8 Dielectric constant imaginary as a function of wavelength for (Ti6Al4V) thin film at different working RF powers.

The variations of the refractive index are versus wavelength in the range 400 nm–1100 nm. It is clear from this figure that the refractive index in general increases with an increase in the thickness, due to the different deposited thicknesses, as shown in Fig. 6.

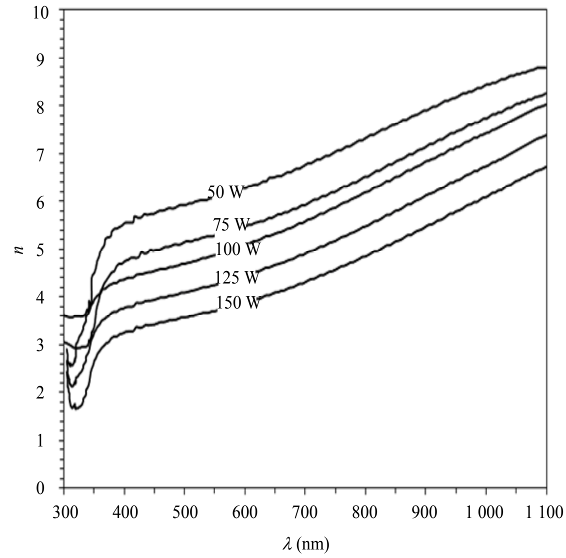

Fig. 9 Refractive index as a function of wavelength for (Ti6Al4V) thin film at different working RF powers.

Table 3 shows the variation of optical parameters at 500 nm wavelength for (Ti6Al4V) films at different RF powers. This table illustrates that T, n, ε_r, ε_i, and E_g decrease with an increase in the RF power while α and K decrease.

Table 3 Optical parameters for (Ti6Al4V) films at the different thicknesses.

Sample	T%	α (cm^{-1})	K	n	ε_r	ε_i	E_g (eV)	Thickness (nm)
50	1.17	55621	0.22	5.92	34.95	2.63	1.54	244.89
75	0.71	61801	0.25	5.16	26.58	2.55	1.44	435.26
100	0.50	66222	0.26	4.68	21.85	2.47	1.39	598.98
125	0.31	72400	0.29	4.09	16.62	2.36	1.34	866.23
150	0.19	78578	0.31	3.57	12.61	2.23	1.23	910.46

4. Conclusions

We investigated the effects of target sputtering power on the structure and mechanical properties of Ti6Al4V film on the glass substrate as deposited by the RF magnetron sputtering technique. The results showed that the structure of the Ti6Al4V films deposited at all the target sputtering powers was polycrystalline with dual structure phases cubic and hexagonal. Films crystallinity and crystalline size increased with an increase in the RF power. AFM data indicated that film roughness was less for samples deposited on the glass substrate at lower sputtering power. It was observed from UV-visible measurements that the absorbance and the extinction coefficient (k) for deposited thin films increased with an increase in the RF power, while other parameters such as dielectric constants and refractive index decreased. The present work can be a guideline for obtaining good quality Ti6Al4V thin films for biomedical applications.

Acknowledgment

We acknowledge the support of the Dept. of Physics, College of Education for Pure Sciences, University of Anbar and Ministry of Science and Technology, Center of Applied Physics, Baghdad, Iraq. We acknowledge Aqeel F. Hasan, Jamal. F. Hamodi, and Mohammed Odaa for their precious help.

References

[1] C. M. Garzón, J. E. Alfonso, and E. C. Corredor, "Characterization of adherence for Ti6Al4V films RF magnetron sputter grown on stainless steels," *D. Reidel*, 1981, 81(185): 175–181.

[2] A. C. Faria, R. C. Rodrigues, A. P. Claro, M. D. G. C. de Mattos, and R. F. Ribeiro, "Wear resistance of experimental titanium alloys for dental applications," *Journal of the Mechanical Behavior of Biomedical Material*, 2011, 4(8): 1873–1879.

[3] S. Roessler, R. Zimmermann, D. Scharnweber, C. Werner, and H. Worch, "Characterization of oxide layers on Ti6Al4V and titanium by streaming potential and streaming current measurements," *Colloids and Surfaces B Biointerfaces*, 2002, 26(4): 387–395.

[4] H. Copete, F. Vargas, and A. Echavarría, "Mediante proyección térmica por combustión oxiacetilénica sobre un sustrato de ti6al4v in vitro evaluation of oxy-fuel thermal sprayed hydroxyapatite coatings onto ti6al4v substrates," *Dyna*, 2013, 10(177): 101–107.

[5] A. E. B. Torres, S. B. Neves, J. C. N. Abreu, C. L. Cavalcante, and D. M. Ruthven, "Single-and multi-component liquid phase adsorption measurements by headspace chromatography," *Brazilian Journal of Chemical Engineering*, 2001, 18(1): 121–125.

[6] S. Roessler, R. Zimmermann, D. Scharnweber, C. Werner, and H. Worch, "Characterization of oxide layers on Ti6Al4V and titanium by streaming potential and streaming current measurements," *Colloids and Surfaces B Biointerfaces*, 2002, 26(4): 387–395.

[7] T. Falcade, L. M. Antonini, T. E. Schmitzhaus, and C. D. F. Malfatti, "Tribological study of ti6al4v coated with amorphous carbon films obtained by electrodeposition," in *15th International Conference on Experimental Mechanics*, Porto, Portugal, pp. 1–11, 2012.

[8] D. H. He, P. Wang, P. Liu, X. K. Liu, F. C. Ma, and J. Zhao, "HA coating fabricated by electrochemical deposition on modified Ti6Al4V alloy," *Surface and Coatings Technology*, 2015, 277: 203–209.

[9] B. Song, S. Dong, B. Zhang, H. Liao, and C. Coddet, "Effects of processing parameters on microstructure and mechanical property of selective laser melted Ti6Al4V," *Materials and Design*, 2012, 35: 120–125.

[10] S. Xu, J. Long, L. Sim, C. H. Diong, and K. Ostrikov, "RF plasma sputtering deposition of hydroxyapatite bioceramics: synthesis, performance, and

biocompatibility," *Plasma Processes and Polymers*, 2005, 2(5): 373–390.

[11] K. V. Dijk, H. G. Schaeken, J. C. G. Wolke, C. H. M. Maree, F. H. P. M. Habraken, J. Verhoeven, *et al*., "Influence of discharge power level on the properties of hydroxyapatite films deposited on Ti6A14V with RF magnetron sputtering," *Journal Biomedical Materials Research*, 1995, 29(2): 269–276.

[12] N. Muslim, Y. W. Soon, C. M. Lim, and N. Y. Voo, "Influence of sputtering power on properties of titanium thin films deposited by rf magnetron sputtering," *ARPN Journal of Engineering and Applied Sciences*, 2015, 10(16): 7184–7189.

[13] M. F. A. Alias, K. M. Rashid, and K. A. Adem, "Optical properties for Ti doped thin ZnO films prepared by PLD," *International Journal of Innovative Research in Science, Engineering and Technology*, 2014, 3(8): 15538–15544.